Field-theoretic study of salt-induced order and disorder in a polarizable diblock copolymer

Douglas J. Grzetic,*,† Kris T. Delaney,*,† and Glenn H. Fredrickson*,†,‡

†*Materials Research Laboratory, University of California, Santa Barbara, California 93106, USA*

‡*Departments of Chemical Engineering and Materials, University of California, Santa Barbara, California 93106, USA*

E-mail: dgrzetic@mrl.ucsb.edu; kdelaney@mrl.ucsb.edu; ghf@ucsb.edu

Abstract

We study a salt-doped polarizable symmetric diblock copolymer using a recently-developed field theory that self-consistently embeds dielectric response, ion solvation energies and van der Waals (vdW) attractions via the incorporation of segment polarizabilities and/or fixed dipoles. This field theory is amenable to direct simulation via the complex Langevin sampling technique, and thus requires no approximations beyond the phenomenology of the underlying molecular model. We measure the shift in the order-disorder transition (ODT) of a diblock copolymer with salt-loading in field-theoretic simulations and observe rich behavior in which solvation, dilution and charge screening effects compete to determine whether the ordered or disordered phase is stabilized. At low salt concentrations, the salt behaves as a selective solvent, localizing into the high-dielectric domains and stabilizing the ordered phase. At high salt concentrations, however, the salt localization vanishes due to charge screening effects and the salt behaves as a non-selective solvent that screens vdW attractions and stabilizes the disordered phase.

Salt-doped block copolymers containing a salt-dissolving block have attracted significant interest in recent decades, primarily for their applications as solvent-free electrolytes in high-performance lithium-based energy devices.[1,2] The addition of salt tends to stabilize ordered phases and swell the salt-dissolving domains, even in some block copolymers that are otherwise disordered at all temperatures when neat.[3] This influence of added salt on the structure of the block copolymer is desirable if the resulting ordered phase contains percolating ion-conducting domains alongside inert domains that provide structural stability,[1] since an effective polymer electrolyte must be capable of resisting the formation of lithium dendrites while maintaining high ionic conductivity. Thus, there has been a considerable effort, both experimentally[3–15] and theoretically,[16–23] to understand the effect of salt-doping on the thermodynamics and structure of these systems.

In the early experimental investigations of salt-doped block copolymers, a dramatic increase in the order-disorder transition temperature T_{ODT} with increasing salt-loading was observed.[3,4] It was proposed that salt-doping caused an increase in the effective χ parameter between the two blocks, which was first explained theoretically by Wang[16] and coworkers[17–19] as originating from an ion's preference to be solvated by the higher-dielectric polymer component. In these theories, a model for the block copolymer free energy was supplemented with a Born solvation description of the ion chemical potential, assuming a linear constitutive relation between the dielectric constant and the polymer composition. A linear increase in χ with salt-loading was predicted[17–19] of the form $\chi = \chi_0 + mr$. Here r is the molar ratio of salt cation to the monomeric species that solvates the ions, and m is a slope that was shown to increase with decreasing ionic radius a, a trend that has also been observed experimentally.[6,17]

More recent experimental work[7,8,14,15] has suggested, however, that χ increases linearly only when r is small, and that it saturates (or in some cases decreases[7]) for larger r. Although it has been demonstrated that such a saturation effect could be explained by incomplete salt dissociation,[17] the experimental evidence of sufficient ion pairing at the relevant

salt concentrations is lacking.[24] The absence of a satisfactory explanation for these higher salt-concentration effects highlights the possible need to consider theoretical treatments that incorporate the relevant charge physics of salt-doping in a more sophisticated manner, e.g., by moving beyond descriptions of the polymeric medium as a dielectric continuum. A recently-introduced polarizable field theory framework[25] enables the construction and simulation of field-theoretic models for complex fluids in which the dielectric properties of the constituent fluid elements (beads) are incorporated by attaching classical Drude oscillators or, alternatively, freely-rotating fixed dipoles to their centers of mass. In addition to granting dielectric response, this incorporation of the polar or polarizable nature of fluid elements embeds dipole-dipole, or van der Waals (vdW), interactions, as well as ion-dipole interactions that generate solvation energies and affect the spatial distribution of ions in systems with dielectric inhomogeneity. Thus, in this framework the charge physics necessary to describe salt localization emerges *self-consistently* as a consequence of the bead dipoles and/or polarizabilities, rather than being imposed *ad hoc* or via uncontrolled approximations. Although such statistical field-theoretic treatments of polar and polarizable charged fluids are not new,[26–29] our version does not rely on simplifying (e.g. mean field) approximations and is amenable to direct simulation via the complex Langevin field-theoretic simulation (CL-FTS) approach. This is crucial, since much of the charge physics described above vanishes in the absence of electrostatic field fluctuations, rendering the mean-field approximation to the polarizable field theory inappropriate or of limited applicability for most problems of interest.

In this Letter, we construct a model for salt-doped polymers out of segments/beads that can each have an embedded classical Drude oscillator, a freely-rotating fixed dipole, or a monopole charge (see Figure 1), based on the prescription outlined in Ref. [25]. The density and charge density of a particular bead is Gaussian-distributed[30] according to $\Gamma_l(\mathbf{r}) = (2\pi a_l^2)^{-3/2} \exp\left(-r^2/2a_l^2\right)$, where a_l describes the 'size' of beads of species l. Beads of the Drude oscillator or fixed dipole type may be characterized by their polarizability[31] $\alpha = \frac{(\delta q)^2}{K}$ or dipole moment $\mu = d\delta q$, respectively, where δq is the magnitude of the partial

charges, K is a spring constant for the oscillator, and d is the length of the dipole rigid link. For simplicity, we consider a generalized model in which the salt is unpolarizable and any specific interactions such as polymer-salt complexation are neglected. Although these chemistry-specific details can be important for the most widely-studied systems, e.g., polymers having lithium-coordinating groups[1] such as polyethylene oxide (PEO), here we focus on the universal aspects of the phase behavior of salt-doped polymers (the effects that will be present for *all* such systems independent of any specific interactions). Our system has volume $\mathcal{V}$ and contains n_p symmetric AB diblock copolymers, modeled as continuous Gaussian chains with degree of polymerization (number of beads) $N = 100$, and $n_+ = n_-$ small molecule cations and anions with valency z. The average density of the system is thus $\rho_0 = (n_p N + n_+ + n_-)\mathcal{V}^{-1}$. The polarizabilities or dipole moments for A and B monomers are chosen to achieve the desired dielectric constants in A-rich and B-rich domains.

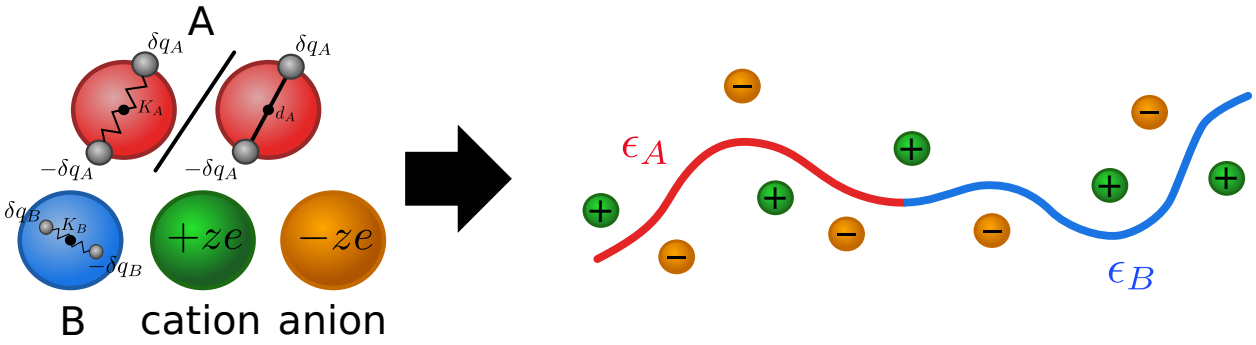

Figure 1: A schematic representation of a symmetric polarizable diblock copolymer doped with a simple small molecule salt. The dielectric properties of the polymer, as indicated in the schematic, are incorporated via the attachment of either classical Drude oscillators or freely-rotating fixed dipoles to the monomeric beads. We consider cases where monomeric species A can be either of the Drude oscillator type (non-polar) or fixed dipole type (polar). Monomer species B is strictly of the Drude oscillator type.

In our model, all charges in the system interact via the bare Coulomb interaction. We include a bare Flory interaction parameter χ_0 acting between monomeric species A and B, which models the contribution to χ from packing entropy differences (recall that the enthalpic contribution to χ, due to vdW interactions, is *automatically generated* in our approach). In addition we include a Helfand compressibility constraint, characterized by the parameter

ζ. Together these interactions contribute the interaction energy $\beta U_{int} = \frac{\zeta}{2\rho_0}\int d\mathbf{r}\,(\check{\rho}(\mathbf{r}) - \rho_0)^2 + \frac{l_B^{(0)}}{2}\int d\mathbf{r}\int d\mathbf{r}'\,\frac{\check{\rho}_c(\mathbf{r})\check{\rho}_c(\mathbf{r}')}{|\mathbf{r}-\mathbf{r}'|} + \frac{\chi_0}{\rho_0}\int d\mathbf{r}\check{\rho}_A(\mathbf{r})\check{\rho}_B(\mathbf{r})$, where $\check{\rho}(\mathbf{r}) = \check{\rho}_A(\mathbf{r}) + \check{\rho}_B(\mathbf{r}) + \check{\rho}_+(\mathbf{r}) + \check{\rho}_-(\mathbf{r})$ is the total microscopic density, $\check{\rho}_c(\mathbf{r})$ is the microscopic charge density (which includes contributions from the partial charges) and $l_B^{(0)}$ is the vacuum Bjerrum length. In this work, we allow for distinct bead sizes a_p and a_s for the polymer and salt species, respectively; this effectively enables us to explore the effects of changing the bare (or unsolvated) ion radius by adjusting a_s. The canonical partition function for this model may be converted from an integral over particle configurations to an integral over field configurations, using standard techniques[32] based on the Hubbard-Stratonovich transformation. The resulting field-theoretic partition function is described in detail in the Supporting Information.

In a recent work[33] we used an analytical one-loop approximation to estimate the contribution to the effective interaction parameter, denoted $\tilde{\chi}$ (where the total $\chi = \chi_0 + \tilde{\chi}$), due to dispersion (vdW) interactions in nonpolar systems with polarizability contrast. We also confirmed the one-loop result by measuring $\tilde{\chi}$ directly in field-theoretic simulations. Following the procedure described in that work, the effect of salt-doping can be straightforwardly traced through the one-loop derivation of $\tilde{\chi}$. In the interest of brevity we do not describe the derivation here, but we simply note that the resulting $\tilde{\chi}$ parameter is given by

$$\tilde{\chi} = \frac{\rho_p}{8\pi^2\epsilon_0^2}\left(\alpha_A - \alpha_B\right)^2 \int_0^\infty dk\, \frac{k^6 \hat{\Gamma}_p^4(k)}{\left(k^2 + \hat{\kappa}^2(k)\right)^2 \hat{\epsilon}^2(k)}, \tag{1}$$

where $\hat{\Gamma}_l(k) = e^{-k^2 a_l^2/2}$ is the Fourier transform of the Gaussian distribution function $\Gamma_l(\mathbf{r})$ for species l, $\hat{\epsilon}(k)$ is the dielectric function for the homogeneous system, and $\hat{\kappa}(k)$ is a charge screening function due to the salt. These screening functions may be estimated by mean-field expressions as $\hat{\epsilon}(k) = 1 + \frac{\rho_p}{\epsilon_0}\left(\alpha_A f + \alpha_B(1-f)\right)\hat{\Gamma}_p^2(k)$ and $\hat{\kappa}^2(k) = \frac{8\pi\rho_s l_B^{(0)} z^2 \hat{\Gamma}_s^2(k)}{\hat{\epsilon}(k)}$, where ρ_p and ρ_s are the average monomer and salt densities, and f is the block fraction of monomeric species A.[34]

Although eq 1 only *estimates* the value of $\tilde{\chi}$ that will be observed in our simulations,

we present it here in order to highlight the sensitivity of $\tilde{\chi}$ to electrostatic screening effects, encoded by its dependence on $\hat{\epsilon}(k)$ and $\hat{\kappa}(k)$. The implication is that as salt is added to the system, the vdW interactions are screened and $\tilde{\chi}$ decreases. Although eq 1 applies strictly to the induced dipole-induced dipole (dispersion) interactions, the permanent dipole-permanent dipole and permanent dipole-induced dipole interactions will both exhibit a similar sensitivity to screening effects. This suggests that although the preferential solvation of salt into the higher-dielectric domains should favor ordering of the block copolymer, this effect must compete not only with any dilution effects but also with the charge screening of $\tilde{\chi}$, both of which favor *disordering*. We will see below, in the simulations of the unapproximated field theory, that the observed phase behavior can be understood in terms of these three effects (preferential solvation, charge screening and dilution).

The complex Langevin field-theoretic simulation (CL-FTS) technique allows us to sample thermodynamic observables without making approximations to the field theory, while avoiding the so-called *sign problem* that plagues the efficiency of more conventional sampling methods (e.g. Monte Carlo) for field theories having complex-valued Hamiltonians. In the interest of brevity, we refer the reader to the literature[32,35–44] for more information on the technical details of this approach, and to the Supporting Information for details of our implementation and numerical parameters. Here we have conducted field-theoretic simulations of the model described above and characterized how the order-disorder transition (ODT) is affected as we vary the salt loading $r = \frac{[+]}{[A]} = \frac{\rho_s}{\rho_p f}$ and the parameter a_s which controls the bare ion radius. The degree of order is characterized using a global orientational persistence order parameter, which is non-zero in the presence of quasi-long-range order.[33,44,45] We consider a dense, weakly compressible melt with average density $\rho_0 = 7.35b^{-3}$, compressibility parameter $\zeta = 1$, and vacuum Bjerrum length $l_B^{(0)} = 32.5b$, where b is the statistical segment length. Throughout, we consider monovalent ($z = 1$) salt, and monomeric species B is modeled as the Drude oscillator type (non-polar) with polarizability volume[46] $\alpha_v^{(B)} = 0.011b^3$, giving $\epsilon_B \approx 2$. For monomeric species A, we consider four cases:[47]

I: Drude oscillator type (non-polar), $\alpha_v^{(A)} = 0.11b^3$, $\epsilon_A \approx 10$,

II: Drude oscillator type (non-polar), $\alpha_v^{(A)} = 0.043b^3$, $\epsilon_A \approx 5$,

III: Drude oscillator type (non-polar), $\alpha_v^{(A)} = 0.011b^3$, $\epsilon_A \approx 2$,

IV: Fixed dipole type (polar), $\mu_A = 0.1be$ (e is the fundamental charge), $\epsilon_A \approx 10$.

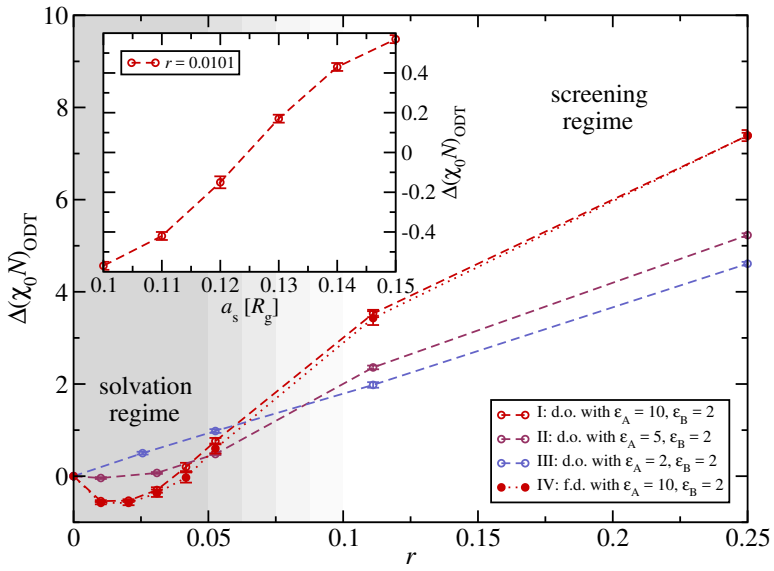

Figure 2: Shift in $\chi_0 N$ at the ODT $\Delta(\chi_0 N)_{\rm ODT}$, relative to the neat diblock copolymer, as a function of salt loading r for case I (red, open), case II (purple), case III (blue) and case IV (red, closed), all with $a_s = a_p = 0.1R_g$. Solvation and screening regimes can be identified for small r and large r, respectively, by comparison with case III which exhibits only dilution effects. In the inset we plot the ODT shift for case I at fixed $r = 0.0101$, as a function of a_s.

The shifts in the ODT as a function of salt loading r from CL-FTS for these four cases are plotted in Figure 2.[48] Case III provides a useful reference case because when $\alpha_A = \alpha_B$ both the preferential solvation effect as well as the vdW-generated $\tilde{\chi}$ necessarily vanish, leaving dilution as the only remaining effect of salt-doping in that case. By contrasting the other cases with case III, we can disentangle the electrostatic effects of salt-doping from the simple monotonic effects of dilution.

The comparison of ODT shifts for cases I, II and IV with case III reveals two regimes, in which the electrostatic (non-dilution) effects of salt-doping in the presence of dielectric

contrast favor either ordering or disordering of the block copolymer at small or large r, respectively, with a crossover occurring in the range $r_c \approx 0.05 - 0.1$. For $r < r_c$, the electrostatic effects favor ordering due to the preferential solvation of salt into high-ϵ domains, consistent with the canonical picture of salt-doped block copolymers; we refer to this as the *solvation* regime. For $r > r_c$, however, the salt favors *disordering*, to a degree that cannot be accounted for by dilution alone. The additional driving force for disorder in this regime is a result of charge-screening effects; thus we refer to this as the *screening* regime. The dielectric contrast clearly affects the magnitude of the electrostatic effects as well as the location of the crossover r_c.

As we mentioned earlier, an important effect that competes with the solvation effect is the charge screening of the vdW-generated $\tilde{\chi}$. In the inset of Figure 2, we plot the ODT shift as a function of a_s, at fixed $r = 0.0101$ for case I. Even for such small r, the resulting ODT shift can be positive or negative depending on a_s, determined by a competition between the ion solvation effect, which dominates when a_s is small and causes a negative ODT shift, and the charge screening of $\tilde{\chi}$, which dominates when a_s is large and causes a positive ODT shift. This indicates that the crossover r_c between the solvation and screening regimes also depends on a_s.

The charge screening of $\tilde{\chi}$ for cases I and II can be estimated using eq 1. For example, in the neat system ($r = 0$) eq 1 gives $(\tilde{\chi}N)_I \approx 3.2$ and $(\tilde{\chi}N)_{II} \approx 0.78$, but at high salt-loading ($r = 0.25$) gives $(\tilde{\chi}N)_I \approx 0.1$ and $(\tilde{\chi}N)_{II} \approx 0.01$. Thus, $\tilde{\chi}$ is *almost entirely screened by the added salt* for large r. Indeed, cases I and II in Figure 2 at $r = 0.25$ exhibit ODT shifts that are larger by $\Delta(\chi_0 N)_I \approx 2.78$ and $\Delta(\chi_0 N)_{II} \approx 0.62$, respectively, than that caused by dilution alone. These values are roughly consistent with (albeit slightly smaller than) our estimates using eq 1, which implies that the competing solvation effect is becoming negligible, or equivalently that the salt behaves as a *non-selective* solvent, at high salt-loading. We find in our simulations that the salt's preference for the A domains is indeed vanishing as r increases. Snapshots of the thermally averaged cation densities from such simulations of

case I are provided for selected values of r in Figure 3; note that the anion and cation behaviors are identical due to the charge symmetry. We see that the salt is localizing into the A domains when r is small, but the localization weakens as r increases and is barely detectable at $r = 0.25$. The effect is quantified in the histograms of cation density which are also provided in Figure 3 for each cation density snapshot.

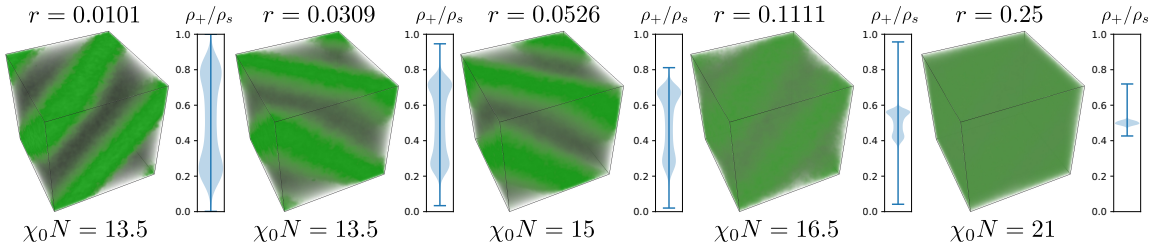

Figure 3: Representative snapshots of the thermally averaged, normalized cation density $\rho_+(\mathbf{r})/\rho_s$, in the lamellar phase, for case I and various r. Each simulation is ran above the ODT in a stable lamellar phase, at the indicated value of $\chi_0 N$. The histogram corresponding to each density snapshot is shown to its immediate right (presented as a violin plot, error bars are the extrema of the distribution). All referenced simulations set $a_s = a_p = 0.1 R_g$.

The vanishing of salt localization, which we see here at large r, is also a charge screening effect. At finite r, an ion's self-energy is screened not only by the dielectric medium but also by the surrounding ion cloud. This effect, which is ignored in theories that assume dilute salt conditions, weakens the salt's preference for higher-dielectric domains. To illustrate this, we consider the ion chemical potential in a salt-doped dielectric fluid. In the one-loop approximation, the electrostatic contribution to the excess chemical potential for an ion in such a medium is given by

$$\beta\mu_i = l_B^{(0)} z^2 \left[\frac{1}{2\sqrt{\pi}\epsilon_M a_s} - 8\rho_s l_B^{(0)} z^2 \int_0^\infty dk \frac{\hat{\Gamma}_s^4(k)}{(k^2 + \hat{\kappa}^2(k))\hat{\epsilon}^2(k)} \right], \tag{2}$$

where $\epsilon_M = \int_0^\infty dk \hat{\Gamma}_s^2(k) \left(\int_0^\infty dk \hat{\Gamma}_s^2(k)/\hat{\epsilon}(k) \right)^{-1}$ can be thought of as the average dielectric constant experienced by an ion.[25] The first term in eq 2 is the infinite-dilution Born energy contribution which has the well-known effect of driving ions to localize into the higher ϵ (A-rich) regions. However, as the salt concentration increases, the second term (a finite-

concentration charge-screening contribution) "washes out" the preference for the higher ϵ domains as the screening of an ion's self-energy becomes dominated by that due to the surrounding ion cloud. As $\rho_s \to \infty$, this latter term cancels the former identically. In

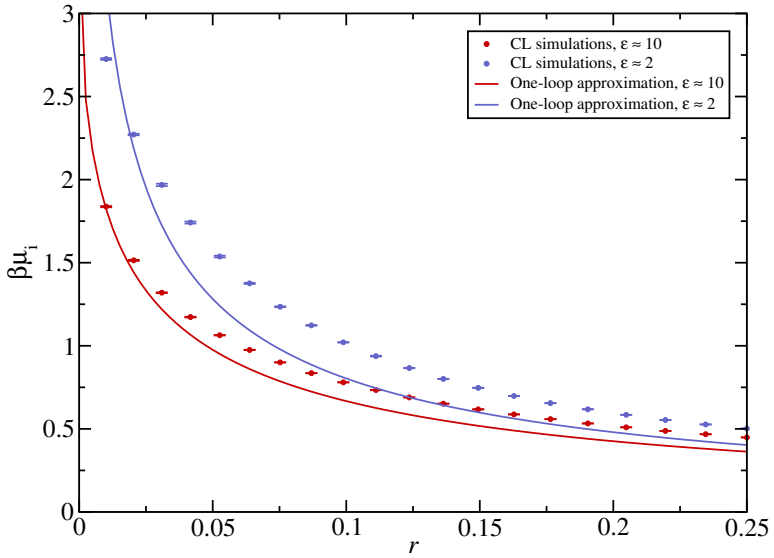

Figure 4: Excess electrostatic chemical potential $\beta\mu_i$ of ions versus salt loading r in a mixture of small molecule salt and polarizable homopolymer with $\epsilon \approx 10$ (red) and $\epsilon \approx 2$ (blue), from CL-FTS (points) and the one-loop approximation (lines, eq 2). Here $a_p = a_s = 0.1R_g$, and all other parameters are the same as in Figure 2.

Figure 4, we plot the electrostatic excess chemical potential $\beta\mu_i$, from CL-FTS, of ions in a mixture of small molecule salt and polarizable (Drude oscillator type) homopolymer, and compare it with eq 2 for the cases where the homopolymer has $\epsilon \approx 10$ (red) and $\epsilon \approx 2$ (blue). Indeed, the difference between μ_i for the two cases of high- and low-ϵ homopolymer, which is significant at small r and indicates the preference of the salt to be solvated by the higher-ϵ species, is clearly vanishing as r increases in a manner that is reasonably well-captured by eq 2.

Our explanation of the main effects of salt-doping does not depend strongly on whether the dielectric properties are embedded using Drude oscillators (non-polar) or fixed dipoles (polar), as indicated by the comparison of cases I and IV in Figure 2. These two cases, which have the same dielectric constants but differ in the polarity of species A nevertheless

exhibit very similar ODT shift behavior. This is despite the fact that there are important differences in the nature of correlations for non-polar and polar fluids, at least some of which have been explored in our previous work.[49] Since such correlation effects are captured by the field-theoretic simulations, evidently they affect the results only quantitatively, at least for the parameters we have considered.

In conclusion, we have studied the phase behavior of a salt-doped polarizable diblock copolymer using a field theory in which the ion solvation physics is embedded self-consistently via the incorporation of monomer polarizabilities and/or fixed dipoles. We have shown that the effect of salt-doping on the phase behavior of the block copolymer is not only determined by the ion solvation energies, but is complicated by dilution effects as well as by electrostatic screening effects due to the ion cloud. The salt behaves as a selective solvent at low salt-loading where it stabilizes the ordered phase as expected (the solvation regime). However, at high salt-loading the salt behaves as a *non-selective* solvent due to charge screening effects, stabilizing the disordered phase (the screening regime). The crossover r_c between the solvation and screening regimes will be sensitive to the details of the specific system, such as the dielectric contrast, ion identity (size, polarizability, etc.) or the presence of any specific interactions (which have been ignored here). It is also possible that the onset of the screening regime will occur for r_c greater than the solubility limit in many systems; nevertheless, even in the solvation regime the effects of charge screening can lead to strong non-linear behavior as seen in Figure 2.

It has been noted in the literature[25,30] that ion-ion interactions cause the ion solvation energy to deviate from the classic Born energy form; despite this, theories for salt-doped polymers have typically ignored the screening influence of the ion cloud. This work thus raises questions regarding the conditions under which it is appropriate to ignore the charge screening effects for this class of problems. In particular, the fact that the salt screens vdW interactions, reducing χ, has not been previously anticipated, despite at least one experimental instance[5] where the enthalpic contribution χ_H (corresponding to our $\tilde{\chi}$) was

seen to reduce dramatically upon salt-doping. Whether or not these screening effects might play a role in the observed non-linearities in χ at higher salt-loading remains as an open question to be explored.

Supporting Information Available

Field-theoretic canonical partition function, numerical details of field-theoretic simulations, order parameter data from simulations, structure factor characterization of salt-doping effects, and dielectric functions measured in simulations.

Acknowledgement

The research reported here was primarily supported by the National Science Foundation (NSF) through the Materials Research Science and Engineering Center at UC Santa Barbara, DMR-1720256 (IRG-2). The CL-FTS methods utilized were developed under support from the NSF Condensed Matter and Materials Theory Program under DMR-1822215. Extensive use was also made of the Center for Scientific Computing from the CNSI, MRL: an NSF MRSEC (DMR-1720256) and NSF CNS-1725797.

References

(1) Young, W.-S.; Kuan, W.-F.; Epps, T. H. Block copolymer electrolytes for rechargeable lithium batteries. *J. Polym. Sci., Part B: Polym. Phys.* **2014**, *52*, 1–16.

(2) Xue, Z.; He, D.; Xie, X. Poly(ethylene oxide)-based electrolytes for lithium-ion batteries. *J. Mater. Chem. A* **2015**, *3*, 19218–19253.

(3) Ruzette, A.-V. G.; Soo, P. P.; Sadoway, D. R.; Mayes, A. M. Melt-Formable Block

Copolymer Electrolytes for Lithium Rechargeable Batteries. *J. Electrochem. Soc.* **2001**, *148*, A537–A543.

(4) Epps, T. H.; Bailey, T. S.; Waletzko, R.; Bates, F. S. Phase Behavior and Block Sequence Effects in Lithium Perchlorate-Doped Poly(isoprene-b-styrene-b-ethylene oxide) and Poly(styrene-b-isoprene-b-ethylene oxide) Triblock Copolymers. *Macromolecules* **2003**, *36*, 2873–2881.

(5) Wang, J.-Y.; Chen, W.; Russell, T. P. Ion-Complexation-Induced Changes in the Interaction Parameter and the Chain Conformation of PS-*b*-PMMA Copolymers. *Macromolecules* **2008**, *41*, 4904–4907.

(6) Wanakule, N. S.; Virgili, J. M.; Teran, A. A.; Wang, Z.-G.; Balsara, N. P. Thermodynamic Properties of Block Copolymer Electrolytes Containing Imidazolium and Lithium Salts. *Macromolecules* **2010**, *43*, 8282–8289.

(7) Huang, J.; Tong, Z.-Z.; Zhou, B.; Xu, J.-T.; Fan, Z.-Q. Salt-induced microphase separation in poly(ϵ-caprolactone)-*b*-poly(ethylene oxide) block copolymer. *Polymer* **2013**, *54*, 3098–3106.

(8) Teran, A. A.; Balsara, N. P. Thermodynamics of Block Copolymers with and without Salt. *J. Phys. Chem. B* **2014**, *118*, 4–17.

(9) Thelen, J. L.; Teran, A. A.; Wang, X.; Garetz, B. A.; Nakamura, I.; Wang, Z.-G.; Balsara, N. P. Phase Behavior of a Block Copolymer/Salt Mixture through the Order-to-Disorder Transition. *Macromolecules* **2014**, *47*, 2666–2673.

(10) Gilbert, J. B.; Luo, M.; Shelton, C. K.; Rubner, M. F.; Cohen, R. E.; Epps, T. H. Determination of lithium-ion distributions in nanostructured block polymer electrolyte thin films by X-ray photoelectron spectroscopy depth profiling. *ACS Nano* **2015**, *9*, 512–520.

(11) Loo, W. S.; Jiang, X.; Maslyn, J. A.; Oh, H. J.; Zhu, C.; Downing, K. H.; Balsara, N. P. Reentrant phase behavior and coexistence in asymmetric block copolymer electrolytes. *Soft Matter* **2018**, *14*, 2789–2795.

(12) Loo, W. S.; Galluzzo, M. D.; Li, X.; Maslyn, J. A.; Oh, H. J.; Mongcopa, K. I.; Zhu, C.; Wang, A. A.; Wang, X.; Garetz, B. A.; Balsara, N. P. Phase Behavior of Mixtures of Block Copolymers and a Lithium Salt. *J. Phys. Chem. B* **2018**, *122*, 8065–8074.

(13) Xie, S.; Lodge, T. P. Phase Behavior of Binary Polymer Blends Doped with Salt. *Macromolecules* **2018**, *51*, 266–274.

(14) Gartner, T. E.; Morris, M. A.; Shelton, C. K.; Dura, J. A.; Epps, T. H. Quantifying Lithium Salt and Polymer Density Distributions in Nanostructured Ion-Conducting Block Polymers. *Macromolecules* **2018**, *51*, 1917–1926.

(15) Sethi, G. K.; Jung, H. Y.; Loo, W. S.; Sawhney, S.; Park, M. J.; Balsara, N. P.; Villaluenga, I. Structure and Thermodynamics of Hybrid Organic-Inorganic Diblock Copolymers with Salt. *Macromolecules* **2019**, *52*, 3165–3175.

(16) Wang, Z.-G. Effects of Ion Solvation on the Miscibility of Binary Polymer Blends. *J. Phys. Chem. B* **2008**, *112*, 16205–16213.

(17) Nakamura, I.; Balsara, N. P.; Wang, Z.-G. Thermodynamics of Ion-Containing Polymer Blends and Block Copolymers. *Phys. Rev. Lett.* **2011**, *107*, 198301.

(18) Nakamura, I.; Wang, Z.-G. Salt-doped block copolymers: ion distribution, domain spacing and effective χ parameter. *Soft Matter* **2012**, *8*, 9356–9367.

(19) Nakamura, I.; Balsara, N. P.; Wang, Z.-G. First-Order Disordered-to-Lamellar Phase Transition in Lithium Salt-Doped Block Copolymers. *ACS Macro Lett.* **2013**, *2*, 478–481.

(20) Qin, J.; de Pablo, J. J. Ordering Transition in Salt-Doped Diblock Copolymers. *Macromolecules* **2016**, *49*, 3630–3638.

(21) Brown, J. R.; Seo, Y.; Hall, L. M. Ion Correlation Effects in Salt-Doped Block Copolymers. *Phys. Rev. Lett.* **2018**, *120*, 127801.

(22) Hou, K. J.; Qin, J. Solvation and Entropic Regimes in Ion-Containing Block Copolymers. *Macromolecules* **2018**, *51*, 7463–7475.

(23) Chu, W.; Qin, J.; de Pablo, J. J. Ion Distribution in Microphase-Separated Copolymers with Periodic Dielectric Permittivity. *Macromolecules* **2018**, *51*, 1986–1991.

(24) Mao, G.; Saboungi, M.-L.; Price, D. L.; Armand, M. B.; Howells, W. S. Structure of Liquid PEO-LiTFSI Electrolyte. *Phys. Rev. Lett.* **2000**, *84*, 5536–5539.

(25) Martin, J. M.; Li, W.; Delaney, K. T.; Fredrickson, G. H. Statistical field theory description of inhomogeneous polarizable soft matter. *J. Chem. Phys.* **2016**, *145*, 154104.

(26) Coalson, R. D.; Duncan, A. Statistical Mechanics of a Multipolar Gas: A Lattice Field Theory Approach. *J. Phys. Chem.* **1996**, *100*, 2612–2620.

(27) Abrashkin, A.; Andelman, D.; Orland, H. Dipolar Poisson-Boltzmann Equation: Ions and Dipoles Close to Charge Interfaces. *Phys. Rev. Lett.* **2007**, *99*, 077801.

(28) Nakamura, I.; Shi, A.-C.; Wang, Z.-G. Ion Solvation in Liquid Mixtures: Effects of Solvent Reorganization. *Phys. Rev. Lett.* **2012**, *109*.

(29) Kumar, R.; Sumpter, B. G.; Muthukumar, M. Enhanced Phase Segregation Induced by Dipolar Interactions in Polymer Blends. *Macromolecules* **2014**, *47*, 6491–6502.

(30) Wang, Z.-G. Fluctuation in electrolyte solutions: The self energy. *Phys. Rev. E* **2010**, *81*, 021501.

(31) We have recently demonstrated[49] that this is only the *bare* polarizability. The true polarizability is renormalized by the electrostatic attraction between the two partial charges. This effect, which is not captured at the mean-field level, is present in the field-theoretic simulations.

(32) Fredrickson, G. H. *The Equilibrium Theory of Inhomogeneous Polymers*; Oxford University Press: Oxford, 2006.

(33) Grzetic, D. J.; Delaney, K. T.; Fredrickson, G. H. The effective χ parameter in polarizable polymeric systems: One-loop perturbation theory and field-theoretic simulations. *J. Chem. Phys.* **2018**, *148*, 204903.

(34) The homogeneous mean-field dielectric function for the case where species A is of the fixed dipole type is given by $\hat{\epsilon}(k) = 1 + \frac{\rho_p}{\epsilon_0}\left(\frac{\beta\mu_A^2}{3}f + \alpha_B(1-f)\right)\hat{\Gamma}_p^2(k)$.

(35) Parisi, G. On Complex Probabilities. *Phys. Lett. B* **1983**, *131*, 393–395.

(36) Klauder, J. R.; Lee, S. Improved complex Langevin method for $(2+1)$-dimensional lattices. *Phys. Rev. D* **1992**, *45*, 2101–2104.

(37) Ganesan, V.; Fredrickson, G. H. Field-Theoretic Polymer Simulations. *Europhys. Lett.* **2001**, *55*, 814–820.

(38) Tzeremes, G.; Rasmussen, K. Ø.; Lookman, T.; Saxena, A. Efficient Computation of the Structural Phase Behavior of Block Copolymers. *Phys. Rev. E: Stat. Phys., Plasmas, Fluids, Relat. Interdiscip. Top.* **2002**, *65*, 041806.

(39) Rasmussen, K. Ø.; Kalosakas, G. Improved Numerical Algorithm for Exploring Block Copolymer Mesophases. *J. Polym. Sci., Part B: Polym. Phys.* **2002**, *40*, 1777–1783.

(40) Düchs, D.; Ganesan, V.; Fredrickson, G. H.; Schmid, F. Fluctuation Effects in Ternary AB + A + B Polymeric Emulsions. *Macromolecules* **2003**, *36*, 9237–9248.

(41) Delaney, K. T.; Fredrickson, G. H. Polymer field-theory simulations on graphics processing units. *Comput. Phys. Commun.* **2013**, *184*, 2102–2110.

(42) Düchs, D.; Delaney, K. T.; Fredrickson, G. H. A multi-species exchange model for fully fluctuating polymer field theory simulations. *J. Chem. Phys.* **2014**, *141*, 174103.

(43) Villet, M. C.; Fredrickson, G. H. Efficient field-theoretic simulation of polymer solutions. *J. Chem. Phys.* **2014**, *141*, 224115.

(44) Delaney, K. T.; Fredrickson, G. H. Recent Developments in Fully Fluctuating Field-Theoretic Simulations of Polymer Melts and Solutions. *J. Phys. Chem. B* **2016**, *120*, 7615–7634.

(45) Qian, H.; Mazenko, G. F. Defect structures in the growth kinetics of the Swift-Hohenberg model. *Phys. Rev. E* **2003**, *67*, 036102.

(46) The polarizability volume α_v can be related to the polarizability α by $\alpha_v = \frac{\alpha}{4\pi\epsilon_0}$.

(47) In the Supporting Information we provide measurements of the dielectric function from CL-FTS for neat homopolymers in cases I-IV.

(48) In general, the addition of salt will result in a finite range of $(\chi_0 N)_{\mathrm{ODT}}$. In the Supporting Information we have characterized the effects of salt-doping by analyzing the structure factor in the disordered phase. We observe the same trends in that analysis, suggesting that the miscibility gap is not significantly influencing our results.

(49) Grzetic, D. J.; Delaney, K. T.; Fredrickson, G. H. Contrasting Dielectric Properties of Electrolyte Solutions with Polar and Polarizable Solvents. *Phys. Rev. Lett.* **2019**, *122*, 128007.

Graphical TOC Entry